Cyclic Sound Intensity and Source separation from NAH measurements on a Diesel engine

Brice Lafon[a], Jerome Antoni[b], Ménad Sidahmed[b] and Laurent Polac[a]

[a]Renault, 67 rue des Bons Raisins, CTR A03 3 37, 92500 Rueil Malmaison, France
[b]Université de Technologie de Compiègne, Centre de Recherche de Royallieu, rue Personne de Roberval, 60200 Compiègne, France
brice.lafon@renault.com

The ranking of noise sources in Diesel engines and the reduction of the noise they radiate is of major concern in the car industry. On the one hand, acoustic imaging techniques allow a spatial localization. On the other hand, source separation methods enable to estimate the contribution of particular sources. However, these two kinds of techniques have rarely been used together.
This paper presents the second part of an original study aiming to couple acoustic imaging techniques with noise source separation methods. More precisely, it deals with Near Field Acoustical Holography (NAH). Concerning the source separation aspect, a cyclic Wiener filter is devised and takes advantage of the cyclostationarity property of engine signals. The idea is to establish a process that provides mean-contribution sound radiation maps and sound radiation movies during a mean engine cycle. Consequently, the breakthrough of this study is a precise estimation and localization in space, in frequency and in time (crankshaft angle) of the occurrence of a specific noise source contribution.

1 Introduction

The engine is the main noise source in a car. The radiated noise results from the mixture of many complex noises produced by various sources (combustion, injection, mechanical shocks…). The reduction of these noises is then an important stake in the car industry. In this context, noise source separation and acoustic imaging are two research fields of great interest. For this reason, RENAULT (French car manufacturer) and the University of Technology of Compiègne (UTC, France) are conducting an original study aiming to couple these techniques. The final objective is to develop an efficient process to detect engine NVH problems at the earliest stage so that they can be quickly solved.

Previously, in the first part [6] of this study, combustion noise separation on Diesel engine radiation was implemented from classical sound intensity measurements. The separation, based on Wiener filtering, was performed by taking advantage of the cyclostationary property of engine signals.

The goal of this paper is to present the second part of this study that aims to overcome the main shortcoming of the previous method: time-consuming measurements. Our method is then applied to Near-Field Acoustical Holography, an acoustic imaging technique faster and more adapted to our industrial context. As previously used in [6], source separation is implemented to complete global radiation maps by specific-source radiation maps such as combustion source and other sources. Furthermore, the exploitation of cyclostationarity enables to define an instantaneous sound intensity estimated during an average engine cycle. Then, radiation movies can be obtained to allow a precise localization of a specific radiation emergence in space, in frequency, and at the same time, in the crankshaft angle domain.

The first part of this paper is dedicated to a brief reminder of the SONAH theory. In a second part, we will tackle the source separation aspect of the study. Finally we will expose in a third part the overall procedure before giving some experimental results in the last part.

2 SONAH Theory

The Statistically Optimized Near field Acoustic Holography (SONAH) theory assumes that the sound pressure at any point of an arbitrary plane ($z = z_c$) in a source free region can be obtained as a weighted sum of sound pressures measured at N points in a measurement plane ($z = z_h$) [3,4,5].

$$p(x,y,z_c) \approx \sum_{n=1}^{N} c_n(x,y,z_c).p(x_n,y_n,z_h) \quad (1)$$

The SONAH procedure aims then to determine the transfer matrix composed of the weights c_n to back propagate the measured sound pressures from the hologram plane to the prediction plane. To provide a good estimation, these weights are required to satisfy a similar equation as Eq.(1), with a finite sub-set of elementary waves instead of the sound pressures,

$$\Phi_{K_m}(x,y,z_c) \approx \sum_{n=1}^{N} c_n(x,y,z_c).\Phi_{K_m}(x_n,y_n,z_h) \quad (2)$$

where the elementary waves Φ_{Km} , (m = 1…M), are defined as follows:

$$\Phi_{K_m}(x,y,z) = e^{j(k_{mx}.x+k_{my}.y+k_{mz}.z)} \quad (3)$$

The regularized least squares solution to the resulting system of equations (1) can be written in matrix notation as:

$$C(x,y,z_c) = (A^H A + \theta^2 I)^{-1}.A^H \alpha(x,y,z_c) \quad (4)$$

where $A^H A$ is an auto-correlation matrix of the set of measured sound pressures, $A^H \alpha$ is a cross correlation matrix between the measured sound pressures and the estimated sound pressures, I is the identity matrix and θ is a regularization parameter.

The final sound pressures in the prediction plane can then be written as follows:

$$P^T(x,y,z_c) = P^T(x,y,z_h).(A^H A + \theta^2 I)^{-1}.A^H \alpha(x,y,z_c) \quad (5)$$

where $P^T(x,y,z_c)$ is the transposed column vector of the sound pressures calculated in the prediction plane and $P^T(x,y,z_h)$ is the same vector with the N sound pressures measured in the hologram plane.

The main advantage of SONAH is the fact that it does not use the discrete spatial Fourier transform used in classical NAH procedure [1]. Therefore, undesirable spatial leakage effects are avoided.

3 Source Separation

3.1 Short overview of existing methods

Concerning noise source separation, two main approaches have been investigated during the last decades: blind source separation (BSS) and Wiener filtering [12]. The first approach is a mathematical method that assumes that the noise sources of interest are statistically independent. The second one requires some a priori knowledge about the source to be separated. For this reason, this method needs the use of an additional signal representing the source of interest.

Wiener filtering was chosen in our study. Nonetheless, the method was performed by taking into account the cyclostationarity property [8,10] fulfilled by engine signals as it is explained in the next part.

3.2 The cyclic Wiener filter

As briefly explained, the aim is to extract from a measured signal $y(t)$, the contribution $x(t)$ associated to a specific source represented by a reference signal $r(t)$ which is coherent to $x(t)$ uncorrelated with the other noises $b(t)$.

$$y(t) = x(t) + b(t) \tag{6}$$

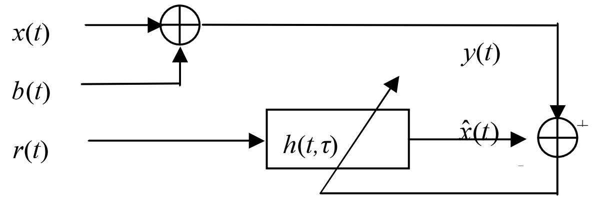

Fig.1 Principle of the cyclic Wiener filtering.

Formally, the estimation of the contribution $x(t)$ is

$$\hat{x}(t) = \sum_{\tau} h(t,\tau).r(t-\tau) \tag{7}$$

The aim is then to estimate the best linear filter $h(t,\tau)$ which, once applied to $r(t)$, will give the best estimation $\hat{x}(t)$ of x(t), minimizing the quadratic error:

$$h(t,\tau) = Arg \min_{h} \mathrm{E}\left\{ \left| y(t) - \hat{x}(t) \right|^2 \right\} \tag{8}$$

It can be specified that in our case, the global noise $y(t)$ is the acoustical pressures measured by the microphones of the array, $r(t)$ is a cylinder pressure signal and $b(t)$ represents what we could qualify as the mechanical noise.

Remark: we outline here that the filter $h(t,\tau)$ is a function of time t, which is not the case for the classical Wiener filter. Here the dependency in time is due to the advantage taken of the cyclostationary property of engine signals [9]. Despite the necessary condition of stable running condition during the measurements, the cyclic Wiener filter goes further than the classical Wiener filter which is based on the assumption of stationarity. Furthermore, here, the fast transient variations (fast non stationarities such as mechanical impacts…) inside an engine cycle can be followed by this periodic and evolutive filter. The estimation of the filter is based on a time synchronous average and not on a temporal average as the classical Wiener filter does (assumption of stationarity).

4 Application to the industrial context

4.1 Measurement conditions

The measurement campains were realised on a dCi engine, in a semi-absorber room at the Renault NVH centre in France. In practice, we used an irregular array with a uniform density of microphones. Furthermore, these measures were conducted under a stable running condition of the engine in order to benefit from the cyclostationarity property of the engine signals as explained above.

4.2 Noise sources of interest

In this study, we tried to separate two major noise sources of a Diesel engine: the combustion noise and the injection noise. The two corresponding Wiener filters were calculated by using a reference signal for each noise source to be separated. As far as the combustion noise was concerned, we used a cylinder pressure signal. Concerning the injection noise, we chose to use a vibration signal measured on the pipes linking the common rail to the injectors.

The separation step was realized in waterfall by taking into consideration one of the four combustion posts. First, the combustion part was extracted from the sound pressures measured by the microphones of the array. After that, the injection part was extracted from the residual pressures obtained after the first separation.

4.3 Process

The proposed process established to obtain the sound radiation maps can be sum up by Fig.2:

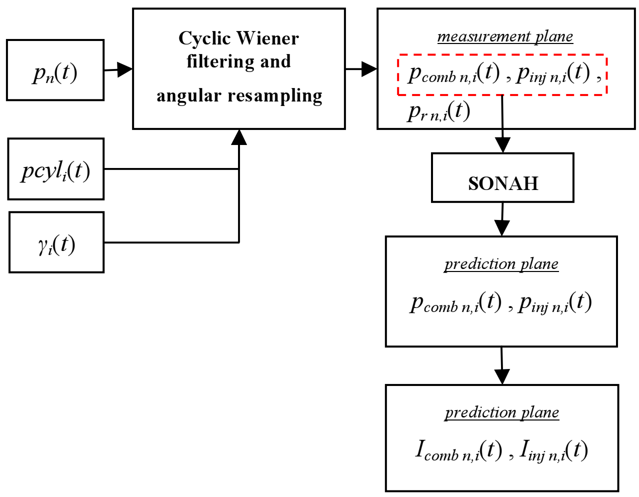

Fig. 2 Process for the calculation of the sound radiation maps.

with:

- $p_n(t)$, the sound pressure measured by microphone n of the array,
- $pcyl_i(t)$, the pressure in cylinder i,
- $\gamma_i(t)$, the vibration signal measured on the pipe common rail - injector i,
- $pcomb_{n,i}(t)$, the combustion part from chamber i on the sound pressure measured by microphone n,
- $pinj_{n,i}(t)$, the injection part from chamber i on the sound pressure measured by microphone n.

5 Experimental results

5.1 Noise source separation results

5.1.1 Example of a single sound pressure signal

Figure 3 is an example of separation realized on a sound pressure signal recorded by one of the microphone of the array. Figure 3.a. shows the first separation result (extraction of the combustion part). Figure 3.b. shows the second separation result (extraction of the injection part). You will notice that the signal on which the second separation is achieved, corresponds to the residual signal from the first separation. Then, for this particular microphone, the combustion part represents 39% of the global recorded sound pressure and the injection part represents 60% of the 61% of residual 1, so the injection part represents 37% of the global sound pressure. The final residual after the two separations represents 24% of the global sound pressure.

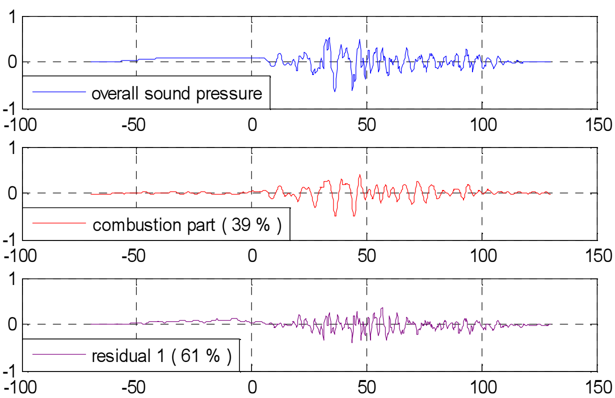

Fig. 3.a. Separation of the combustion noise:
a) overall sound pressure,
b) combustion part,
c) intermediary residual.

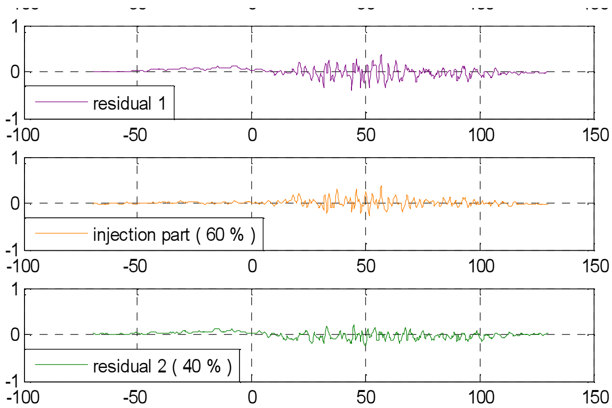

Figure 3.b. Separation of the injection noise:
a) intermediary residual from the first separation,
b) injection part,
c) final residual.

5.1.2 Extension to the entire array

The separation process is achieved at each measurement point. The contribution parts are then back propagated in a prediction plane corresponding most often to the source plane. The sound intensity in the source plane is then calculated from the contributions in order to draw sound radiation maps corresponding to the parts of the combustion noise and the injection noise on the global noise radiated by a specific face of the engine. Figure 4 shows the separation results for the over face of a dCi engine in a specific 1/3-octave frequency band. Sound levels have been normalized and adjusted in order to show clearly the contribution of each analysed source.

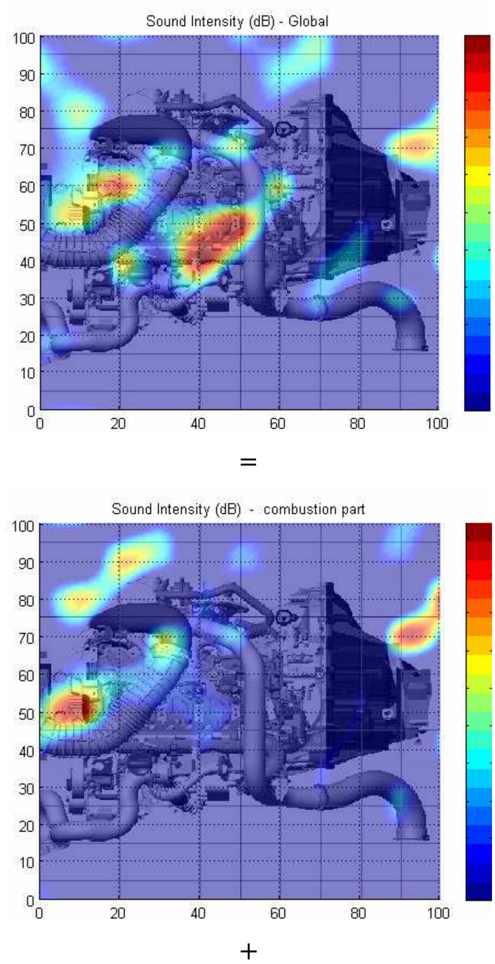

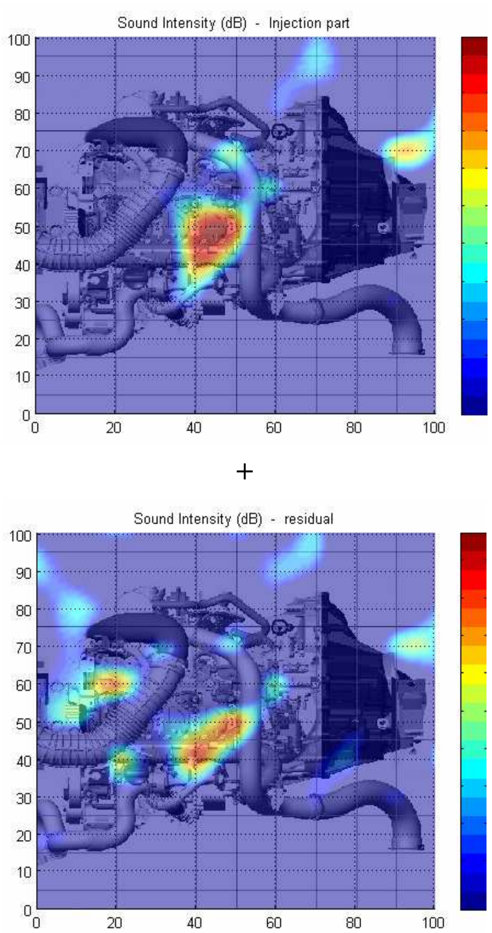

Fig. 4 Separation results for an over face engine: a) global sound intensity, b) combustion part, c) injection part, d) residual.

5.2 Cyclic sound intensity and sound radiation movies

Another aim of this study was to estimate the sound intensity in the time-frequency domain during an average engine cycle T_{cycle} to clearly identify at which instant inside the engine cycle a certain component radiates. A cyclic sound intensity was defined in [6]. It was calculated once more by taking advantage of the cyclostationarity property of engine signals measured under stable running conditions of the engine.

Figure 5 shows some results from classical sound intensity measurements. The upper part of the figure corresponds to a sound intensity map for a specific frequency band and at a precise crankshaft angle whereas the lower part corresponds to the cyclic sound intensity during the average engine cycle for a specific measurement point localized on the upper map by the black square. The radiation map is updated by moving the red line cursor along the cycle. We get then a sound radiation movie during the engine cycle (from 0° to 720° crankshaft).

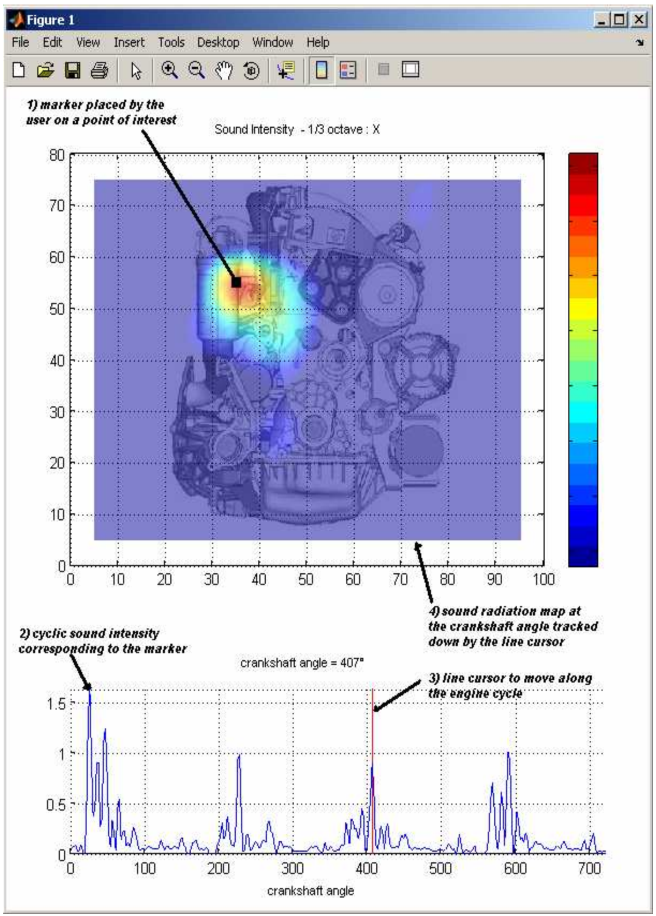

Fig. 5. Sound radiation movie and cyclic sound intensity.

6 Conclusion

To conclude on this second part of our initial study, we succeeded in solving the main shortcomings encountered in the first part with classical sound intensity measurements. NAH measurements and SONAH algorithm are less time consuming and then more adapted to our industrial context. The association of this acoustic imaging technique with source separation based on Wiener filtering provides additional information that can ensure a more effective NVH diagnosis at the earliest stage of the design. Furthermore, new sound radiation movies can be obtained to precisely notice the angle, inside an engine cycle, at which a particular noise is emerging and from which part of the engine, the corresponding sound radiation is coming. The radiation can then be localized in space, in frequency and in crankshaft angle at the same time.

References

[1] E.G. Williams, "Fourier Acoustics – Sound Radiation and Nearfield Acoustical Holography". Academic Press, London, UK, 1999.

[2] E.G. Williams, "Fourier Acoustics: Uncovering the origins of sound". Proceedings of ICSV 11th, St. Petersburg, Russia, july 5-8, 2004.

[3] J. Hald, "Patch Near-field Acoustical Holography using a new statistically optimal method". B&K Technical Review n° 1 – 2005.

[4] J. Hald, "Combined NAH and Beamforming using the same array". B&K Technical Review n° 1 – 2005.

[5] J. Hald, "STSF- a unique technique for scan-based Near-field Acoustic Holography without restrictions on coherence". B&K Technical Review n° 1- 1989.

[6] B. Lafon, J. Antoni, "Cyclic Sound Intensity for noise separation Diesel powertrain unit radiations". Proceedings of InterNoise 07, Istanbul, Turquey, august 28-31, 2007.

[7] W.A. Gardner, "Cyclostationarity in communications and signal processing". IEEE Press (1994).

[8] J. Antoni, Apport de l'échantillonnage angulaire et de la cyclostationarité au diagnostic par analyse vibratoire des moteurs thermiques. Ph.D Thesis of the National Polytechnic Institute of Grenoble (2000) (in French).

[9] J. Antoni, M. Sidahmed and R. Boustany, "Separation de sources sur moteur F9Q par traitement du signal". Technical Report from the University of Technology of Compiègne for Renault, (2004) (in French).

[10] J. Antoni, R. Boustany, F. Gautier and S. Wang, "Source Separation in Diesel engines with the cyclic Wiener filter". Proceedings of EuroNoise 2006, Tampere, Finland, 30 May – 1 June 2006.

[11] C. Renard, L. Polac, J.C. Pascal and S. Sahraoui, "Extraction of vibration sources in Diesel engines". Proceeding of 11th International Congress on Sound and Vibrations – ICSV11, St Petersburg, July 5-8, 2004.

[12] M. El Badaoui, J. Danière, F. Guillet and C. Servière, "Separation of combustion noise and piston slap in diesel engine by cyclic Wiener filtering". Mechanical Systems & Signal Processing, 19(6), 1209-1217 (2005).

[13] S. Wang, C. Chalu and F. Gautier, "Optimization of combustion noise of modern Diesel engines for passenger cars". SAE 2007-01-2379.